Journal of Engineering Science and Technology
Vol. XX, No. Y (Year) PPP - QQQ

COMPARISON OF NUMERICAL AND EXPERIMENTAL RESULTS FOR OVERTOPPING DISCHARGE OF THE OBREC WAVE ENERGY CONVERTER

A. YAZID MALIKI[1], M. AZLAN MUSA[1], AHMAD M. F.[1,]*, ZAMRI I.[1], OMAR Y.[2]

[1]School of Ocean Engineering, Universiti Malaysia Terengganu, Malaysia
[2]Faculty of Mechanical Engineering, Universiti Teknologi Malaysia, Malaysia
* Corresponding Author: fadhli@umt.edu.my

Abstract

OBREC is the latest innovation of overtopping wave energy converter (WEC) which is coalesced with the rubble mound breakwaters. The acquisition of wave overtopping in a front reservoir and consequently releasing process through turbine is the concept of energy production in OBREC. The physical scale model studies of overtopping discharge of the OBREC have recently been done by previous researcher in wave flume at Aalborg University. This paper demonstrates the overtopping behavior of OBREC device using a VOF method with capabilities to solve RANS equation in the numerical suite *Flow3D*. The purpose of this research is to validate the overtopping discharge performance of the numerical model against the experiments of the OBREC. Based on the observation, the results have shown a good agreement between the validation and physical experiment.

Keywords: Wave energy converters; Wave overtopping; CFD modeling.

1. Introduction

Global dependency towards fossil fuels increased by 0.8% in 2014, showing a remarkable decline compared to 2013 (+2.0%). The consumption increased for all fuels except nuclear power, and oil remained the world's leading fuel consumption [1]. Persistant increment of fossil fuel consumption every year stimulates intensive researches on renewable energy resources as an alternative energy sources to be fully utilized. One of the renewable energy sources most progressively reviewed so far is ocean wave energy. The global technical potential of wave energy is estimated at 11,400 TWh per year and it can create up to 10% of global energy need per year sustainably [2].

Nomenclatures

B_r	Reservoir width, m
d_w	Height of sloping plate, m
	the toe of the structure, m
F	Fetch length, m
g	Gravity acceleration, m/s^2
H_{mo}	Incident significant wave height in the frequency domain at
h	Water depth at the toe of the structure, m
$L_{m-1,0}$	Deep water wave length referenced to $T_{m-1,0}$, m
$q_{reservoir}$	Average overtopping discharge in the reservoir, l/s/m
R_c	Crest freeboard of crown wall; i.e. the vertical distance between the crest of the vertical wall and the still water level, m
R_r	Crest freeboard of front reservoir; i.e. the vertical distance between the crest of the sloping plate and the stillwater level, m
R_r^*	Relative crest freeboard of front reservoir (R_r / H_{m0}), [-]
$T_{m-1,0}$	Spectral incident energy wave period at the toe of the structure, s

Greek Symbols

ΔR_c	$R_c - d_w$, m
γ	Peak enchancement factor, [-]

Abbreviations

AWS	Archimedes Wave Swing
CFD	Computational Fluid Dynamics
JONSWAP	Joint North Sea Wave Project
OBREC	Overtopping BReakwater for Energy Conversion
RANS	Reynolds Average Navier-Stokes
R&D	Research and development
SSG	Sea-wave Slot-cone Generator
VOF	Volume of Fluid
WECs	Wave Energy Converters

Many researches attempted to fulfill global energy needs by exploring ocean wave technologies recently but they are still unable to reach the level of technical maturity. Based on International Patent Cooperation Treaty publication in 2013 [3], about 80 registered patents for R&D in ocean energy technologies come from WECs. Nevertheless, only a few devices have reached fullscale prototype deployments such as Pelamis in UK, and AWS in Portugal but others remain in R&D stage, with prototype system or model demonstrated in an actual working environments [3].

Technically, researchers tend to focus on structural design and hydraulic efficiency on WECs devices without identifying survivability of these models during storm, and causing many WECs unable to operate much longer physically. Therefore, in order to attract attention from policy makers and investors, WECs products itself must be designed with capabilities for commercially viable. Several barriers in commercialising WECs devices were highlighted in [3] including technical

fundamentals, economic pressures, environmental and social issues and infrastructural practicalities. Industrial investment only can be obtained by researchers or developers only if they can proved that their WECs devices are improving performances, reducing costs and validating wave energy technologies [4].

The fundamental target of WECs is to provide competitive energy cost [3] for global needs as an alternative source of energy. But most of researches are unable to be economically viable since the costs of constructing, deploying, maintaining and testing large prototypes during extreme storm is relatively high [3,8] and in fact, WECs energy transfer efficiency is relatively lower than other renewable energy source [7]. To resolve those issues, researchers had started to develop hybrid concept of WECs devices. The primary objective of developing the hybrid concept is to be competitive with the other renewable energy devices [5]. Nowadays, there are several hybrid concepts proposed by researchers in combining WECs with other renewable energy technologies such offshore wind turbine or aquaculture farms, which is also known as multiplatform concepts. These concepts were believed to benefit by sharing implementation costs, reducing operation and management costs, and had environmental sustainability [8].

Therefore in order to achieve those benefits, and as an initial step to commercialize WECs, some researchers have been pioneering the model scale experiments of hybrid concept by integrating WECs into breakwaters. Since the construction costs of breakwaters is relatively high [9], adopting WECs into breakwater could being a two-pronged approaches, in addition of providing a calm basin for ships and to protect harbour facilities [10], it also can produce electricity.

One of the most recent hybrid concept known as OBREC is integrated with breakwater has physically modeled and tested by Vicinanza [1–3] at Aalborg University, Denmark in 2012. OBREC is an integration between a traditional rubble mound breakwater and a front reservoir to store the wave overtopping from the incoming wave to produce electricity. It was designed to extract energy via low head turbines, using the difference in water levels between reservoir and the mean sea water level. The present studies of the OBREC focuses on hydraulic performance and impacts of wave loads on the structure and rubble mound breakwater respectively. Moreover, the OBREC design formulae was also presented intentionally for the development of a first prototype by engineers.

Problems related to hydraulics and sedimentation engineering have previously often been solved by the used of physical models. However, physical models are costly and time-consuming, compared to Computational Fluid Dynamics (CFD) models. [13] The overall aim of the present study is to investigate the feasibility of using CFD for large scale simulations of WECs in general. Our specific purpose is to validate the performance of the numerical model against the experiments of the OBREC presented in [1–3].

2. Experimental Works

In 2012, the preliminary studies was pioneered by [11] with general aims to contribute towards sustainable development of coastal infrastructures which benefits economic and environmental by integrating WECs and breakwaters. The first 2D model of the OBREC was modeled by using a scale of 1:30 and was tested at Aalborg University in a large wave flume, 1.5 m wide and 25 m.

The laboratory model tests have analysed the values of the overtopping performance involving two models namely OBREC and traditional rubble mound breakwater with a crown walls. The preliminary results have shown the loading on the vertical wall and overtopping on the rear side can be reduced by installing front reservoir.

In the latter study [12] in 2013, from the same experimental results obtained by the year 2012, the author had aims to study on wave loadings acting on sloping and vertical wall constituting the structure. The OBREC which was modeled by using 34º frontal slope and were tested by two different height of front sloping wall in 2012, namely 0.075 m and 0.125 m. In predicting pressure distribution on OBREC internal reservoir and vertical wall, the authors reported that modification of Takahashi's design formulae [14] is needed to make it valid for OBREC application.

Eventually, the most current studies of OBREC has been published in 2014 [5] with aims to complete the analysis on OBREC geometric parameter variations. The differences between the model tests carried out in 2012 and 2014 are the structural parameters and also the measurement used for the wave overtopping in the front reservoir. In 2012 tests, the usage of ramp at the front reservoir had caused an increase in the overtopping rear the structure, and thus by placing a parapet on top of the crown wall had reduced an average overtopping by 50-60% [1,2]. In 2014 tests, more details on hydraulic performance of the OBREC were reported in [5].

3. CFD Modelling

Computational Fluid Dynamics or usually shortened as CFD is a method of simulating a flow process in which standard flow equations such as the Navier-Stokes and continuity equation are discretized and solved for each computational cell. Using CFD software is in many ways are similar to setting up an experiment. If the experiment is not set up correctly to simulate a real-life situation, then the results will not reflect the real-life situation [15].

In a modern applications of CFD, there are numerous branches of physical science that can be relies on the applications of CFD including heat transfer, radiation, nuclear reaction, electromagnetic field, oceanography, vascular medicine and etc. Based on fluid mechanics field, the general CFD studies included nonlinear waves, viscous effects, green water effects, slamming loads, wave breaking, etc. [16] In recent times, researchers have progressively study on the wave hydraulics behaviors and structural design performance mostly in the aspect of wave overtopping discharges by using various types of CFD softwares which can be found on [18–26]

Nevertheless, only several researchers have exploited the use of FLOW-3D in their researches on wave behaviors over a coastal structure including Dentale who mostly studied on the reliability of FLOW-3D as a design tool by investigating interaction between wave motion (regular and irregular waves) with several types of coastal structures [21,25,26], Cavallaro [21] had studied on the reliability of 3D numerical simulation over overtopping of rubble mound breakwater and also Vicinanza [17] had studied on structural response of SSG WECs device using irregular waves. The results from those mentioned researches proved that FLOW-

3D is one of an innovative CFD software with ability to simulate real-life situation. FLOW-3D is based on the RANS which designed for turbulance simulation and Volume of Fluid (VOF) for free surface computation methods [25].

4. Methodology of Experiment

In every CFD case, validation is used to assess how accurately the computational resuts compare with the experimental data. For that reason, in geometrical construction using CAD program, all these geometries have been reconstructed using structural design parameters same as previous experiment. The workflow diagram that provides summary of this CFD studies is given in Fig. 1.

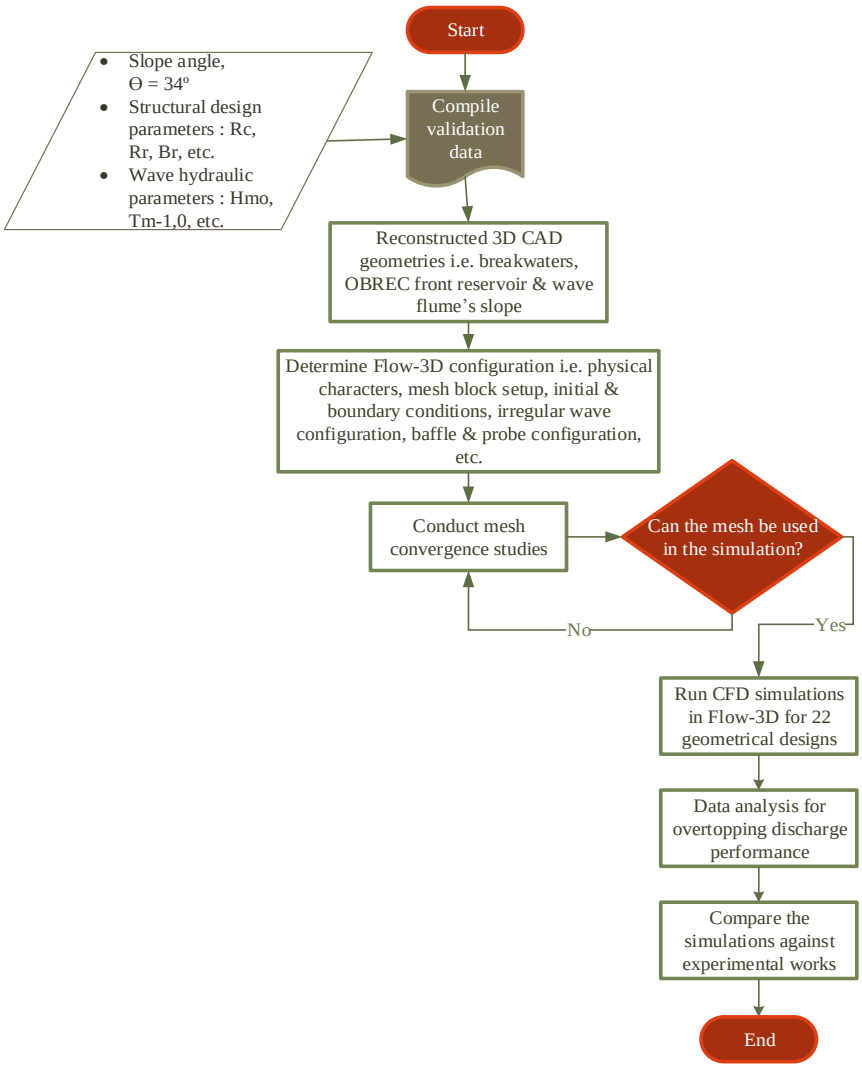

Fig. 1. Workflow diagram of the CFD studies.

Based on 1:30 (Froude Scaling) model scale parameters in Table 1, as to ensure significant result is obtained, 22 geometrical parameters of the OBREC for extreme and production conditions cases were constructed by using 3D CAD softwares. A slope of $\theta = 34°$ was positioned at the OBREC sloping front ramp and were tested for different freeboards. The structural design parameters of each case was adjusted based on minimum and maximum values of experimental geometries in Table 1. Thus, breakwaters, both submerged and emerged, are numerically reconstructed by overlapping individual blocks under the conditions of gravity, collision and friction, according to the real geometry, very much like in the case of laboratory test model.

Since the OBREC and breakwater geometries for each cases was defined, subsequently these geometric files are exported into the CFD system namely FLOW-3D codes. A numerical wave flume was set up in order to carry out the numerical simulation based on typical experimental arrangements, which consists of the lengths 1 m in x direction, 25 m in y direction and 1.5 m in z direction. From the initial bottom of the flume (at 0 m in y direction) was characterized without the presence of a paddle as such in physical experiment and followed by a distance of 6.5 m towards a 1:98 slope until reaching to the model. The computational domain is divided into two sub-domains (Figure 2), the general mesh block domain represents the area where the fluid is flowing and while, the local mesh block domain represents the area of structural geometry to be located.

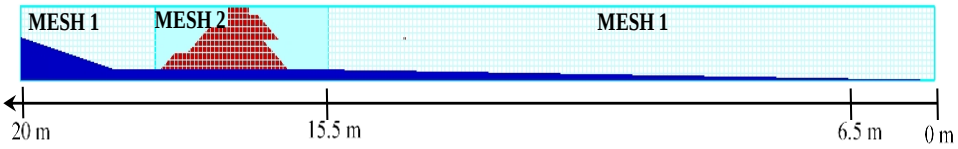

Fig. 2. Computational boundary meshing for numerical wave flume.

In FLOW-3D codes, the baffle acts as the flux surface diagnostical tool [15] in computing flow rate quantities for a simulation. Therefore, in order to compute overtopping discharge at front reservoir of the OBREC, a baffle has being configured vertically just after a sloping ramp at the front reservoir in y direction until the end of z direction in computational domain. While a history probe in FLOW-3D functions to compute different parameters at the location of the probe [15]. Thus, 3 history probes were used to be function as the wave gauge by installing near the toe of the breakwater in order to measure free surface elevation of incoming waves. The location at which historical probes were installed was suggested by Klopman and van der Meer [26] and the incident and reflected spectra were determined using the approach of Mansard and Funke [27]. Wave pressure distribution was not measured in this numerical works but it will be investigated in the next paper. In addition, the configuration locations of history probes are similar to physical experiment but the difference of interval between history probes could not be retain approximately as was in experiment.

4.1. Irregular wave configuration

The former experimental studies use JONSWAP wave spectrum (random waves) with the peak enchancement factor, γ is 3.3. In order to numerically simulate and

validate against the physical experiment, JONSWAP random wave energy spectrum has been obtained from Kofoed [28] containing approximately 100 waves. The energy spectrum file has two columns, where the left one is a series of angular frequencies of waves (in rad/time), and the right column is the corresponding energy values [15]. The JONSWAP spectrum is designed for fetch-limited sea and was developed by the Joint North Sea Wave Project [29]. It can be read as:

$$E(\omega) = \frac{\alpha g^2}{\omega^5} exp\left[-\frac{5}{4}\left(\frac{\omega_p}{\omega}\right)^4\right]\gamma^{exp\left[-\frac{(\omega-\omega_p)}{2\sigma^2\omega_p^2}\right]} \quad (1)$$

where, $\omega_p = 22\left[\frac{g^2}{U_{10}F}\right]^{1/3}$ is the angular frequency at the spectrum peak; $\alpha = 0.076\left[\frac{U_{10}^2}{Fg}\right]^{0.22}$ is a scaling parameter; g is the gravitational acceleration; γ indicates the peak enchancement factor by the range of $1 \leq \gamma \leq 7$ and typically $\gamma = 3.3$; the value of σ is determined by $\sigma = 0.07$ for $\omega \leq \omega_p$, and $\sigma = 0.09$ for $\omega \geq \omega_p$; U_{10} denotes the wind speed 10m above the mean sea level and F signifies the fetch length. [15]

A latter step is to identify boundary condition for each sub-domains, where for general domain block contains virtual waves flow and subsequently, from starting point of y direction was declared as wave boundary by selecting JONSWAP wave energy spectrum file for generating wave onwards, and at the end of y direction was declared as outflow boundary which is useful when modeling linear surface waves exiting at this boundary [15] and for the rest of boundary conditions were declared as symmetry except for the surface boundary at the z axis has been integrated with pressure boundary in order to characterize the time history of hydrodynamics force acting on the OBREC. The details of boundary conditions set-up has been presented in Fig. 3.

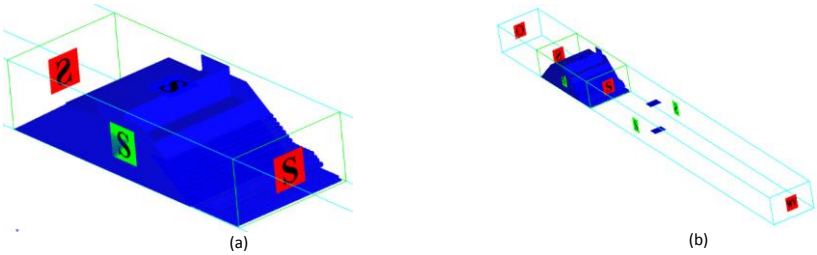

Fig. 3. Boundry condition on: (a) the OBREC mesh block, (b) the wave flume mesh block.

Fluid region has been set up to define fluid initial condition of the overall numerical set-up, the water level in front of the structure has been fixed at 1.5 m, whereas the rearside has been kept a level higher than the height of outflow pipe of the OBREC. However, low head turbine is not attached to the structure. A RNG turbulence closure have been chosen. A time step of 0.01s has been employed. Finish time has been made up to be 300s. A series of 22 numerical simulations were carried out by using several machines built with Processor Type Intel(R) Core(TM) i7 CPU, 2.67GHz with the RAM capacity is 16Gb. Numerical simulation tested geometries and wave characteristics are reported in Table 1, and numerical simulation dimensionless tested parameter ranges are reported in Table 2.

Mesh convergence studies has been conducted by using 7 meshing parameters to estimate the most appropriate meshing for all geometries in order to reduce computational burdens. The details on the parameters and the results of mesh convergence studies were given in Table 3, Figures 4 and 5.

Table 1. Wave characteristics and reservoir geometrical parameters for OBREC (Production).

Test (Simulation ID)	h [m]	H_{m0} [m]	$T_{m-1,0}$ [s]	R_c [m]	R_r [m]	B_r [m]
Production						
A1 (Min) -	0.27	0.08	1.48	0.27	0.105	0.415
A11 (Max)		0.059	1.65		0.155	0.488
Extreme						
A12 (Min) -	0.3	0.081	2.33	0.2	0.075	0.415
A22 (Max)	0.34	0.052	1.51	0.24	0.125	0.488

Table 2. Dimensionless tested parameter ranges for OBREC.

Test	$H_{m0}/L_{m-1,0}$	H_{m0} / h	R_r / H_{m0}	$B_r/L_{m-1,0}$	$h/L_{m-1,0}$	$\xi_{m-1,0}$
Extreme	0.04	0.27	0.93	0.21	0.15	6.9
(Min-Max)	0.03	0.17	2.39	0.27	0.19	5.6
Production	0.019	0.27	1.31	0.09	0.07	4.4
(Min-Max)	0.023	0.198	2.61	0.16	0.12	5.7

4.2. The governing equations for data analysis

The most important part of the OBREC studies is to understand the potential energy that could be harness from that device. Thus, the main factor that playing a vital role in the OBREC potential energy production is the wave overtopping in the front reservoir. The overtopping at the front reservoir of the OBREC which previously studied by Vicinanza [5], has been tested by the prediction formula from [30] and [31] (Eqs. (1) and (2), however it was unable to predict overtopping rate with sufficient accuracy at the OBREC structure [5]. The prediction formula seems to overestimate in interpreting results. The prediction formula in [30,31] gave similar results and plotting upper limit on graph as both were developed for smooth impermeable slopes. A relatively good estimation was obtained from existing prediction formula by [32] which was introduced two coefficients factor; γ_f, reduction factor for slope roughness and γ_β, reduction factor for oblique wave attack. A regression analysis was used by [5] to select an equavalent roughness reduction factors for OBREC, and the most fitting of the data was obtained using an average roughness coefficient of $\gamma_{f,OBREC} = 0.7$. The non-dimensional average overtopping discharge in the reservoir, $q^*_{reservoir}$ and relative crest freeboard, R^*_r are presented in Eqs. (2) and (3), respectively.

$$q^*_{reservoir} = \frac{q_{reservoir}}{\sqrt{g.H^3_{mo}}} \quad (2)$$

$$R_r^* = \frac{R_r}{H_{mo}} \tag{3}$$

The non-dimensional wave-structure steepness, $S_{Rr}{}^*$ (see Eq. 4) has been introduced by [5] as a new parameter that was included into a new prediction formula of the OBREC device for determining the non-dimensional average overtopping discharge in the front reservoir, $q^*_{reservoir}$ as was expressed in Eq. (5).

$$S_{Rr}{}^* = R_r^* \frac{R_r}{L_{m-1,0}} \tag{4}$$

$$q^*_{reservoir} = 39 - 2.4 \frac{d_w}{\Delta R_c} . e^{-\left(31.7+17.7\frac{d_w}{\Delta R_c}\right).S_{Rr}{}^*} \tag{5}$$

The range of application of Eq. (5) is $0.64 < d_w/\Delta_{Rc} < 1.35; 0.0123 < S^*_{Rr} < 0.202$ based on physical experiment presented in [5].

In real-time operational deployments and modeling studies, accurate estimation of wave height and period are becoming increasingly important in coastal environment. Typically in physical studies of wave and current, data were collected using acoustic Doppler technology wage gauge to calculate directional wave spectra and records surface elevation time series for zero-crossing and spectral analysis. The same methodology has been applied using numerical simulation where free surface elevation can be tracked down by using history probe in FLOW-3D codes. Hence, the locations at which the probes are configured is important for the purpose of dividing into incident and reflected waves using an approach of [27]. So as was suggested by [26], three probes were configured near the toe of the breakwater. All those methods were used by Vicinanza [1,3] during physical experiment of the OBREC modeling tested in Aalborg University laboratory.

Historically, zero-crossing analysis and spectral methods have been widely used to estimate wave parameters such as $H_{1/3}, H_{mo}, H_{1/10}, H_{max}, T_z$ and T_p. The statistical theory of random signals to narrow band ocean waves were formerly applied by [33] which had demonstrated that wave heights posses a Rayleigh distribution. Thus from Rayleigh distribution, the narrow band spectra can be expressed as:

$$H_{1/3} = 1.416 H_{rms} = (1.416)\left(2\sqrt{2m_o}\right) = 4.005\sqrt{m_0} = H_{m_o} \tag{6}$$

The significant wave height, $H_{1/3}$ is an average of the $1/3$ highest wave is estimated using zero-crossing analysis of the surface elevation in time series. From the spectral analysis, an energy based significant wave height namely, H_{m_o}, which can be roughly defined as four times the square root of the sea surface variance, m_0 (see Eq. 6). In general, [34] had suggested that $H_{1/3}$ is typically 90 to 100% of H_{m_o} between a range of $(1 < H_{m_o}/H_{1/3} < 1.11)$.

5. Results and Discussion

The comparison has been made between volumetric overtopping discharge of the OBREC in front reservoir against time as presented in Table 3 for mesh convergence study. In this case, a total of 7 tests have been run using the same geometric design by the different meshing sizes.

Table 3. Mesh convergence studies parameters.

Test ID	Fine (Mesh Block 1)	Coarse (Mesh Block 2)	Ratio	Average overtopping discharge (m^3/s)
B1	0.01	0.02	1:2	0.070
B2	0.009	0.018	1:2	0.309
B3	0.008	0.016	1:2	0.319
B4	0.007	0.014	1:2	0.366
B5	0.006	0.012	1:2	0.386
B6	0.005	0.01	1:2	0.385
B7	0.004	0.008	1:2	0.390

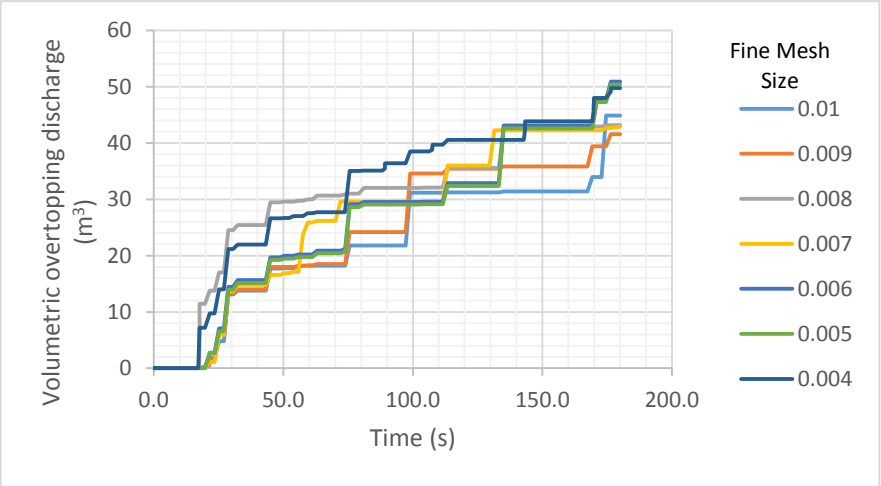

Fig. 4. Mesh convergence studies of volumetric overtopping discharge against time.

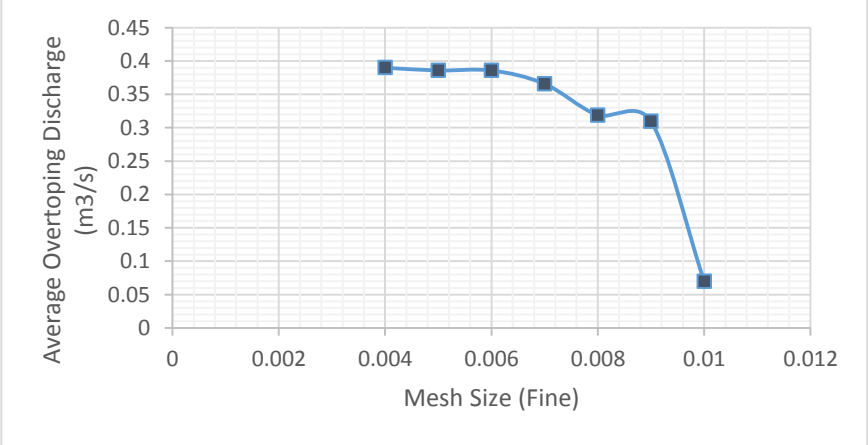

Fig. 5. Mesh convergence studies of average overtopping discharge for specific meshing size.

The graph in Figure 4 shows the increasing amount of volumetric overtopping discharge in the reservoir over time. The comparison has been made by different 'fine' mesh sizes to investigate the most appropriate meshing to be used in futher simulations. Thereby in the graph, a simulation of using the mesh size of 0.006 shows a significant increase of volumetric overtopping discharge in front reservoir compared with other mesh sizes over simulation period indirectly positively reacts to stability in processing the simulations. Subsequently, the result from Figure 5 has strengthen the fact that the used of 0.006 mesh size is encouraging to be applied in further investigation where, the highest average overtopping discharge obtained within the graph is quite consistent between three mesh sizes namely 0.004 until 0.006. The mesh sizes are perfectly suitable to be applied in further research, but the most prefered (coarse domain) mesh for all computations was chosen to be made up of 0.01 size of cell, 20x0.03x0.6 m, and while the (fine domain) mesh was 0.005 size of cell, 2.5x0.03x0.6 m.

The results of the analyses in this numerical simulation focus on wave overtopping behavior in the front reservoir by neglecting the studies on wave reflection and wave loading acting on the structures. The reason at which wave overtopping behavior was taken into account for the current numerical validation is to to look into the probabilities that futher studies can be proceeded for adopting OBREC in Malaysia. In this research, the results from the analyses are compared to the data of physical experiment for validation purpose through the qualitative observation on the graphs as regards to a similar trends within the aspects of data distribution, gradient of the graph, correlation between the variables, trendline, etc. The observation results can be used to support physical modeling, as a useful tool in preliminary design phase to allow a selection of design alternatives. The snapshot in Figure 6 has shown waves behavior in the front reservoir for validation tests.

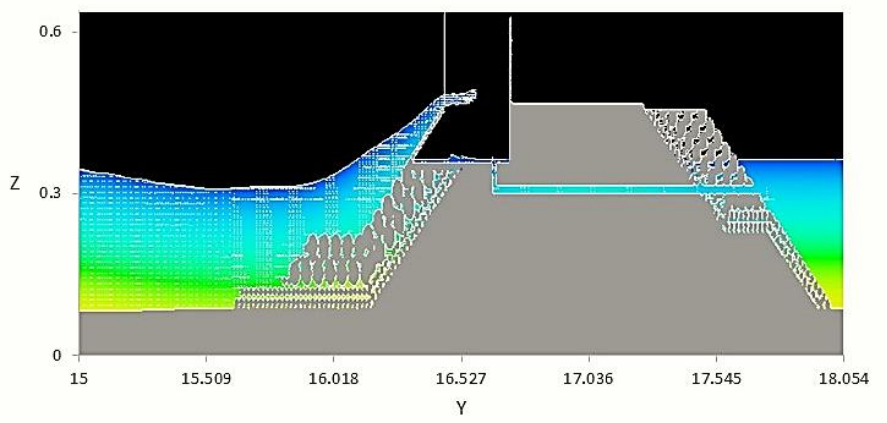

Fig. 6. Overtopping waves behavior in the front reservoir by vector direction

According to Vicinanza [5] in 2014, the main focusing of the physical model tests is to obtain reliable information on hydraulic performance based on the "production" wave conditions. Thus, the numerical simulation was carried out to validate overtopping discharge performance of OBREC based on the well proven result of physical experiment. The graph in Figure 8 has shown a strong negative

correlation between experimental and simulation results of Dw Low and Dw High. The OBREC with overall identical dimensions used in simulation was based on experiment, but the overall R_r^* is slightly increased when compared with experiment. In fact larger overtopping was expected in simulation due to the usage of smooth type of rock shape in numerical breakwater. In general, the graph has shown an encouraging relationship between both results indirectly proving the simulation is importance to obtain preliminary result before the physical experiment is carried out.

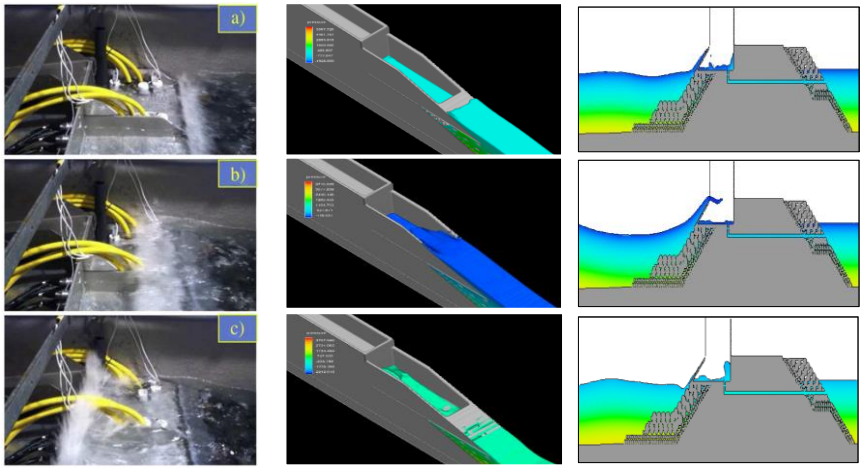

Fig. 7. Comparison of waves run-up, overtopping and reflection behaviors in front reservoir between experimental against numerical 3D & 2D

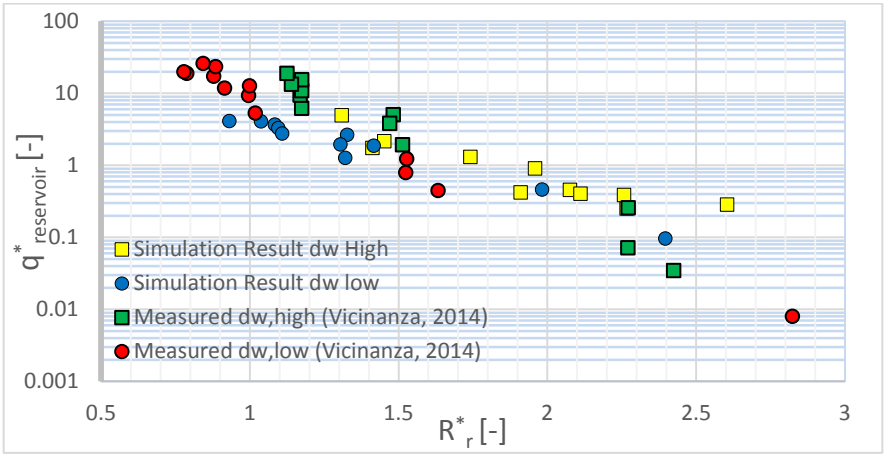

Fig. 8. Simulated result of non-dimensional average front reservoir overtopping discharge vs experimental results.

The main difference of the results between simulated and experimental is due to the probability of difficulties in defining the real situation during numerical simulation configuration. Typically, this behavior may be due to the sampling

effect associated with the limitedness of the wave series employed (approximately in the range of 80 to 90), but may also have a more rigorous physical explanation [17]. The result obtained for the non-dimensional average overtopping discharge in the reservoir, $q^*_{reservoir}$ and relative crest freeboard, R^*_r suggested that the described methodology could be used successfully to analyze the phenomena of interaction between wave overtopping and the OBREC devices.

Futhermore, the latter result in Figure 9 is a comparison between simulated and physical experiment which was calculated using a new prediction formulae of Vicinanza [5] in Eq. (5). The range of application employed in Eq. (5) during experimental work is between $0.64 < d_w/\Delta_{Rc} < 1.35; 0.0123 < S^*_{Rr} < 0.202$ which was assumed to be fitted with experimental result. The same prediction formulae also was used with the simulated results to investigate whether by using different level of crest freeboard of the front reservoir in the range of $0.105 < R_r < 0.155$ (representing Dw high) for "production" wave condition and also in the range of $0.075 < R_r < 0.125$ (representing Dw low) for "extreme" wave condition (refer to Table 1), the same inclination pattern of the graph could be obtained.

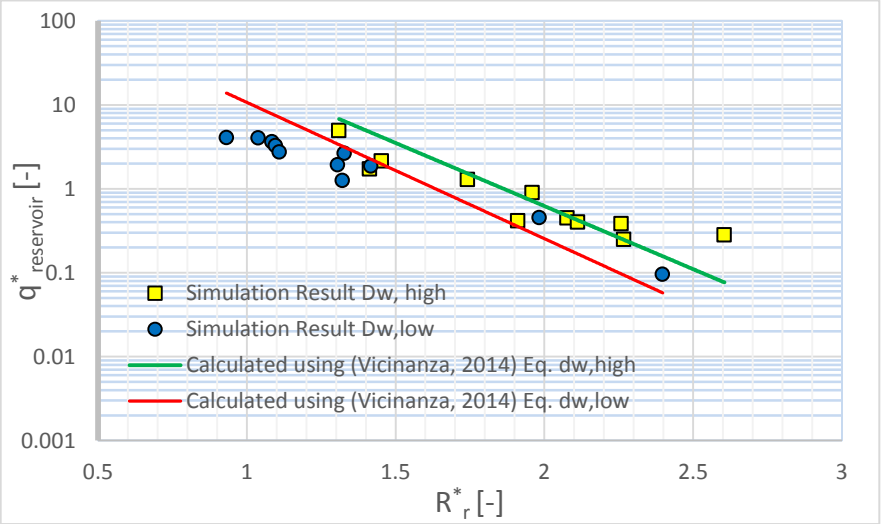

Fig. 9. Comparison of using Vicinanza Eq. (5) (new prediction formulae of $q^*_{reservoir}$) against simulation results

The graph presented in Figure 9 has shown a negative correlation associated with simulated results between non-dimensional average overtopping discharge in the reservoir, $q^*_{reservoir}$ and relative crest freeboard, R^*_r. It is obvious as the crest freeboard of the front reservoir is increase, the overtopping rate in the front reservoir declines, and vice versa. Hence, the result has shown a good agreement between simulated result of Dw,low and Dw,high against experimental results. The distribution of simulated data plotted in the graph is within the application range used by Eq. (5) during physical model tests.

The given graph in Figure 10 illustrates the non-dimensional wave overtopping rate in the front reservoir of the simulated result by comparing with

physical experiment and different existing design formulae by Van der Meer (1998), Kofoed (2002), EurOtop (2007) and Victor and Troch (2012).

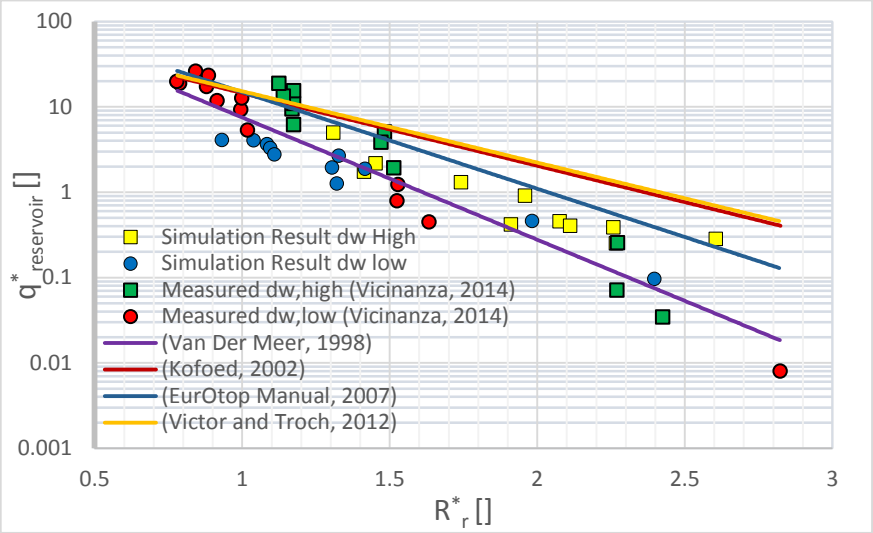

Fig. 10. Comparison between different design formulae, physical experiment and numerical simulation results.

Based on the coefficient of determination, R^2 in statistical modeling corresponded to Figure 10, simulated result of Dw,low has shown about 96% of the variation in non-dimensional average overtopping discharge in the reservoir, $q^*_{reservoir}$ is associated with variation in relative crest freeboard, R^*_r and whilst, about 86% of the variance is associated with regression line in simulated result of Dw,high. Meanwhile, it indicates that both regression lines of the simulated results of the Dw,low and Dw,high is fitted with the simulated data. Moreover in comparison by the different design formulae among several researchers and also well proven model test result by Vicinanza [5], the simulated results showing a good relation where the dots are tightly clustered around the other regression lines. Nevertheless, there is significance difference related to the slope presented by Dw,low and Dw,high of simulated results compared with other results which demands for further explanation and might end up to uncertainty.

There are several possible explanations to the discrepancy and one of which is regarding to the number of waves employed during simulations. It is impossible to employ a large number of waves through numerical simulation because the time consumed for simulation work is relatively high. In some cases, Vicinanza [17] in particular who has studied structural response of SSG WEC using FLOW-3D previously had employed around 100 waves for his numerical simulation works. Besides, Eskilsson [16] who had studied overtopping discharge of the Wave Dragon WEC using OpenFOAM has taken 1000 hours in running irregular sea state simulations of using 128 cores computer processors. Another important reason which renders the variance may be ensued through the uncertainty in terms of porrosity that applied on armour layer in breakwater during preprocessing customization in FLOW-3D configuration. The current RANS/VOF simulation was

carried out by using porous media approach as such applied in Cavallaro [21], where each of tested numerical breakwater is constructed by overlapping individual blocks under the condition of gravity thus shaping the structure in accordance to real physical experiment parameters. However, the shape of rock used for the armour layer block mound in numerical breakwater is reproduced by using a sphere without properly formed just as the real natural stones in physical model tests. In consequence will affect the overtopping rate in front reservoir of the simulated results since the surface roughness is not taken into account. Generally, the gap existed between simulated results and experimental results was identified and compromised by the previous studies [21,25,26] that using FLOW-3D.

6. Conclusions

Numerical modelling is used to support the design of the OBREC, in a configuration with a rubble mound breakwater and a front reservoir. This paper presents the results of a validation study for overtopping discharge of the OBREC by using different relative crest freeboard in line with berm modification. Experiments in the wave flume of Aalborg University were used to validate the modelling accuracy and compare the efficiency between the different models. Thus the outcomes of the CFD simulation showed a similar trends when compared with the experimental data based on qualitative observation on the graphs. Several difference are highlighted and demands for further investigation. In particular, the areas for improvement in this studies is related to the number of the waves employed, porrosity upon the existence of breakwater, and surface roughness used on rock mound. Although presently, there are several issues in query, but a cost benefit analysis by using CFD simulation to study on overtopping discharge of the OBREC has given adequate outcome. In an another word, overtopping discharge estimated using RANS/VOF method of FLOW-3D is sufficient to provide accurate preliminary prediction result rather than using laboratory test which is costly and time consuming.

References

1. Vicinanza, D.; Stagonas, D.; Nørgaard, J.H.; and Andersen, T.L. (2012). Innovative breakwaters design for wave energy conversion. *33rd International Conference on Coastal Engineering*, 1-12. Santander, Spain.
2. Vicinanza, D.; Harck Nørgaard, J.; Contestabile, P.; and Lykke Andersen, T. (2013). Wave loadings acting on overtopping breakwater for energy conversion. *Journal of Coastal Research*, 29(65), 1669-1674.
3. Vicinanza, D.; Contestabile, P.; Quvang Harck Nørgaard, J.; and Lykke Andersen, T. (2014). Innovative rubble mound breakwaters for overtopping wave energy conversion. *Journal of Coastal Engineering., Vol. 88*, 154–170.
4. British Petroleum (2015). BP statistical review of world energy June 2015. Retrieved December 1, 2015, from http://scholar.google.com.
5. Bollmann, M.; Bosch, T.; Colijn, F.; Ebinghaus, R.; Froese, R.; Güssow, K.; Khalilian, S.; Krastel, S.; Körtzinger, A.; Langenbuch, M.; Latif, M.; Matthiessen, B.; Melzner, F.; Oschlies, A.; Petersen, S.; Proelß, A.; Quaas, M.; Reichenbach, J.; Requate, T.; Reusch, T.; Rosenstiel, P.; Schmidt, J. O.;

Schrottke, K.; Sichelschmidt, H.; Siebert, U.; Soltwedel, R.; Sommer, U.; Stattegger, K.; Sterr, H.; Sturm, R.; Treude, T.; Vafeidis, A.; van Bernem, C.; van Beusekom, J.; Voss, R.; Visbeck, M.; Wahl, M.; Wallmann, K.; and Weinberger, F. (2010). Living With the Oceans. *World Ocean Review: Living with the oceans, Vol. 1*.

6. Mofor, L.; Goldsmith, J.; & Jones, F. (2014). Ocean Energy: Technology Readiness, Patents, Deployment Status and Outlook. *International Renewable Energy Agency (IRENA)*, Abu Dhabi.
7. Magagna, D., & Uihlein, A. (2015). 2014 JRC Ocean Energy Status Report. *European Commission Joint Research Centre*.
8. Wan Nik, W.; Sulaiman, O.; Rosliza, R.; Prawoto, Y.; and Muzathik, A. (2011). Wave energy resource assessment and review of the technologies. *International Journal of Energy and Environment, Vol. 2, No. 6*, 1101–1112.
9. Ding, S.; Han, D.; and Zan, Y. (2014). The Application of Wave Energy Converter in Hybrid Energy System," 936–940.
10. Vosough, A. (2011). Wave Energy. *International Journal of Multidisciplinary Sciences and Engineering (IJMSE) Vol. 2, No. 7*, 60–63.
11. U.S. Army Corps of Engineers (1981). Low Cost Shore Protection: A Guide for Engineers and Contractors.
12. S. Takahashi (2002). Design of vertical breakwaters. *Port and Airport Research Institute - Japan, Vol. 1996, No. 34*.
13. Olsen, N. (1999). Computational fluid dynamics in hydraulic and sedimentation engineering.
14. Mansard, E. P. D.; and Funke, E. R. (1980). The Measurement of Incident and Reflected Spectra Using a Least Squares Method. *Proceedings of 17th Conference on Coastal Engineering*, Sydney, Australia, 154–172.
15. Klopman, G.; and van der Meer, J. W. (1999). Random Wave Measurements in Front of Reflective Structures. *Journal of Waterway, Port, Coastal, and Ocean Engineering, Vol. 125, No. 1*. 39–45.
16. Takahashi, S.; Tanimoto, K.; and Shimosako, K. (1994). Wave Pressure on Perfortorated Wall Caisons. *Proceeding of International Conference on Hydro-Technical Engineering for Port and Harbor Construction*, 747–764.
17. Flow Science (2012). FLOW-3D Documentation. Release 10.1.0. Flow Science, Inc.
18. Eskilsson, C.; and Palm, J. (2015). CFD study of the overtopping discharge of the Wave Dragon wave energy converter. *In Proc. 1st International Conference of Renewable Energies Offshore. ASCE, 2015*.
19. Vicinanza, D.; Dentale, F.; and Buccino, M. (2015). Structural Response of Seawave Slot-cone Generator (SSG) from Random Wave CFD Simulations. *In Twenty-fifth International Ocean and Polar Engineering Conference*.
20. Vanneste, D.; and Troch, P. (2015). 2D numerical simulation of large-scale physical model tests of wave interaction with a rubble-mound breakwater. *Journal of Coastal Engineering, Vol. 103*, 22–41.
21. Dentale, F.; Donnarumma, G.; Carratelli, E. P.; Giovanni, V.; Ii, P.; and Sa, F. (2014). A new numerical approach to the study of the interaction between wave motion and roubble mound breakwaters. *In Proceedings of the 7th*

International Conference on Engineering Mechanics, Structures, Engineering Geology (EMESEG '14), 45–52. Salerno, Italy: WSEAS Press.

22. Nam, B. W.; Shin, S. H.; Hong, K. Y.; and Hong, S. W. (2008). Numerical Simulation of Wave Flow over the Spiral-Reef Overtopping Device. *In Proceedings of the Eighth ISOPE Pacific/Asia Offshore Mechanics Symposium*, 262–267.
23. Cavallaro, L.; Dentale, F.; Donnarumma, G.; Foti, E.; Musumeci, R. E.; and Carratelli, E. P. (2012). Rubble Mound Breakwater Overtopping: Estimation of the Reliability of a 3D Numerical Simulation. *Journal of Coastal Engineering, No. 85*, 4–5.
24. Yu, Y. H.; and Li, Y. (2013). Reynolds-Averaged Navier-Stokes simulation of the heave performance of a two-body floating-point absorber wave energy system. *Journal of Computers and Fluids, Vol. 73*, 104–114.
25. Dentale, F.; Donnarumma, G.; and Carratelli, E. P. (2014). Numerical wave interaction with tetrapods breakwater. *International Journal of Naval Architecture and Ocean Engineering*, *Vol. 6*, 1–13.
26. Dentale, F.; Donnarumma, G.; and Carratelli, E. P. (2012). Wave Run Up and Reflection on Tridimensional Virtual Breakwater. *Journal of Hydrogeology & Hydrologic Engineering*, *Vol. 8*, 1–8.
27. Hirt, C. W.; and Nichols, B. D. (1981). Volume of fluid (VOF) method for the dynamics of free boundaries. *Journal of Comp. Physics, Vol. 39*, 201–25.
28. Kofoed, J. P. (2005). Model Testing of the Wave Energy Converter Seawave Slot-Cone Generator. *Journal of Hydraulics and Coastal Engineering, Vol. 18*.
29. Hasselmann, K.; Barnett, T. P.; Bouws, E.; Carlson, H.; Cartwright, D. E.; Enke, K.; Ewing, J. A.; Gienapp, H.; Hasselmann, D.E.; Kruseman, P.; Meerburg, A.; Muller, P.; Olbers, D. J.; Richter, K.; Sell, W.; and Walden, H. (1973). Measurements of Wind-Wave Growth and Swell Decay during the Joint North Sea Wave Project (JONSWAP). *Ergnzungsh. zur Dtsch. Hydrogr. Zeitschrift R., Vol. A(8), No. 80*.
30. Victor, L.; van der Meer, J. W.; and Troch, P. (2012). Probability distribution of individual wave overtopping volumes for smooth impermeable steep slopes with low crest freeboards. *Journal of Coastal Engineering, Vol. 64*, 87–101.
31. Kofoed, J. P. (2002). *Wave Overtopping of Marine Structures - Utilization of Wave Energy*. Ph.D. Thesis. No. 24. Department of Civil Engineering, Aalborg University, Denmark.
32. van der Meer, J. W. (1998). Wave run-up and overtopping. *Chapter 8 In: Pilarczyk, K.W. (Ed.), Seawalls, Dikes and Revetments*. Balkema, Rotterdam.
33. Longuet-Higgins, M. S. (1952). On the statistical distribution of the heights of sea waves. *Journal of Marine Research, Vol. XI, No. 3*, 245–266.
34. Tucker, M. J.; and Pitt, E. G. (2001). Waves in Ocean Engineering. *Elsevier Ocean Engineering Book Series, Vol. 5*.